Mechanisms and Machine Science
Print ISSN: 2211-0984 | Electronic ISSN: 2211-0992
Volume 15 : 1, 2023

Human Activity Recognition via Optimized Deep learning with Improved Hierarchy of Skeleton[1]

Kumari Priyanka Sinha
Department of Computer Science and Engineering
Nalanda College of Engineering, Chandi, Bihar, India
Prabhat Kumar
Department of Computer Science and Engineering
National Institute of Technology Patna, Bihar, India

Abstract

One of the vast topics is the recognition of human activity that focuses on recognizing a person's particular movement or action based on the sensor data. Due to issues like partial occlusion, background clutter, variations in look, viewpoint, scale, lighting, detecting the human activities from video sequences is a difficult process. A multimodal activity recognition system is required for several applications like human-computer interface, video surveillance systems, and robots for the recognition of human activity. This paper intends to introduce a new human activity recognition model and it involves three process like "(1) Pre-processing, (2) Feature Extraction and (3) Classification". The pre-processing of input data is done via background subtraction. The pre-processed data are subjected to extract the features, in which an improved hierarchy of skeleton, weighted bag of Visual words, and Local Texton XOR patterns are extracted. Based on the extracted features, the classification process takes place, in which the Optimized Deep Belief Network (DBN) is exploited. For more precise detection, the weight of DBN is optimally tuned via proposed Poor and Rich with Deer Optimization (PRDO) model. Finally, performance of the presented model is computed over the conventional techniques with respect to various performance metrics.

Keywords

Human Activity Recognition; Feature Extraction; Deep Belief Network; Classification.

I. INTRODUCTION

Understanding the human activities and context is a key component that enables and supports a wide range of context-aware applications, such as user behavior modeling for advertising and marketing,

[1]Address Author Correspondence to Kumari Priyanka Sinha at kumaripriyankas.phd18.cs@nitp.ac.in
Accepted: 28 March 2023 / Published online: 13 April 2023

home monitoring and health care, context-based personal assistants, video surveillance, etc. One of the important topics in the above applications is video-based Human Activity Recognition (HAR) [9] [10]. In the context of video content analysis, HAR is a high-level meaningful description of a scene corresponding to the recognizable set of objects that interact over time and space. Objects are marked regions in video frames, and their temporal and spatial relationships among the objects get varied in the frames [11] [12]. The complexity of human activity recognition resides in the the temporal and spatial variation, complexity of human behaviours and the video streams uncertainty that has occurred due to the video resolution, dynamic environment, and the computational complexity of the video-based detection task. Activity recognition offers a high description of activities in videos by combining input from several low-level modules, including motion/object/person detection, image enhancement, template/background updation, background model generation, and object tracking, actually results in a sequence of feature vectors for extracting the activity [13] [14].

Compared to single-layer strategies, it recognize and represent low-level behavior as a subset of image sequence, the hierarchical techniques are determined by designing a difficult scene, the semantics and inherent structure of difficult behavior , which requires reasoning techniques and higher-level representation [15] [16]. The capability to detect larger-level activities with higher complicated framework is a key benefit of hierarchical methods over single-layered systems. Hierarchical methods are particularly well suited to a semantic-level evaluation of object-to-object and/or human-to-human interactions, and also complicated group activities. Hierarchical methods represent the activities with less training and recognize them more effectively through numerous high-level activities [17] [18]. Furthermore, the high-level activities enable the incorporation of human information into recognition systems. Further, the human information in the system consists of combined high-level activity with semantically relevant sub-activities and/or describing their connections. One of the most difficult issues for these applications is bridging the semantic gap among low-level human comprehension and high-level human understanding [19]. For example, in HAR, a composite activity is decayed into simple behaviour such as actions and interactions, and into poses and gestures. This problem could be further characterized as: how to design an adequate hierarchical framework to assess semantic ordering and immediately build the associated reasoning system on the basis of hierarchical system to complete the desired job [20] [21].

HAR [22] with mobile sensor devices have traditionally characterized as a multivariate time series classification issue. A fundamental stage in solving the problem is feature extraction, that might involve some statistical characteristics of the raw signal or incorporating some cross-formal coding. These heuristic characteristics are normally employed in time series data analysis. Nevertheless, researchers may create a multi-layer deep structure in the Deep Learning (DL) model [42] [43] to automatically extract the important characteristics [23]. A DL algorithm [40] [41] [45] [44] could train data both unsupervised and supervised, and it has a major impact on graphical data processing. Furthermore, the representation of time series characteristics has recently received a lot of attention. The most effective method is to express the characteristics as visual signals [24]. Time series is re-coded into pictures to allow machines for image identification in computer vision using supervisory and non-hyper-

visual learning approaches. This technique has been demonstrated to be more successful in classification, speech recognition, and radio frequency identification [25].

The following are the key contributions of the accepted model:

- Extracts improved hierarchy of skeleton, weighted bag of Visual words, and Local Texton XOR patterns features from the input.
- Introduces a Poor and Rich with Deer Optimization (PRDO) Algorithm for training the Deep Belief Network (DBN) via tuning the optimal weights.

In this paper, the reviews on HAR model are determined in section II. Overview of the adopted HAR framework is determined in section III. Pre-processing and feature extraction phase for HAR is portrayed in section IV. Classification via optimized DBN classifier is portrayed in section V. Section VI describes weight optimization via poor and rich with deer optimization algorithm. Section VII depicts the result and discussion. At the end, the conclusion of this paper is depicted in section VIII.

II. LITERATURE REVIEW

A. Related works

In 2020, Hairui et al. [1] have suggested a hierarchical structure-based framework and methodology for HAR through the knowledge-based approaches. In particular, this method created a hierarchical framework for expressing the composite behavior as a synthesis of gestures and low-level actions based on its semantic significance. Using data-driven machine learning approaches, this framework was converted into “formal syntactical logical formulas” and ruled to detect the composite behavior assuming the identified lower-level activities. The current study presented a potential architecture and application demonstration of symbolic reasoning and machine learning integration.

In 2020, Manan et al. [2] have implemented an ensemble technique of Multi-Label Classification (MLC), as well as a comprehensive experimental assessment of the Classifier Chain method in the field of HAR. Four alternative classifiers were developed as basis classifiers including Bernoulli Nave Bayes(NB), Decision Tree(DT), Logistic Regression(LR), and K-nearest neighbor(KNN), and a comparative evaluation was performed for this multi-label classification technique. Moreover, for the activity recognition issue, the “Majority Voting Ensemble Classifier technique” was created. On publicly accessible ARAS datasets, all of these models were assessed using a variety of analytical measures. Experiment findings revealed that the Classifier Chain technique effectively tackled the problems of this complicated task.

In 2019, Zhen et al. [3] have investigated a novel Deep Neural Network (DNN) model for HAR based on various sensor inputs to aid data-driven and informed decision making. The suggested architecture transforms sensor data time series into images and utilizes these converted images to preserve the defining features for HAR. Moreover, wearable sensor-based HAR was accomplished employing computer vision algorithms for image recognition based on imaging time series. In terms of F1-value and accuracy rate, the results indicated that the suggested technique outperformed other competitive techniques.

In 2019, Hazar et al. [4] have implemented a new method for HAR in video sequences collected by UAVs. There were two steps in the proposed method: an inference phase and an offline phase. Along with these two steps, a scene stabilization step was completed. Using a convolutional neural network, the offline phase attempts to create a human activity framework and the human/non-human framework. In order to identify the human actions, the inference step takes use of the previously constructed models. The key contribution of this research work resides in the adaptation of convolutional neural network (CNNs) for detecting the humans. Furthermore, human activities were classified using two different scenarios: immediate and complete classification of video frames. Based on simulated results of the suggested techniques on the UCF-ARG dataset, researchers were able to validate not only these contributions, but also the performance of adopted work.

In 2020, Pham et al. [5] have introduced SensCapsNet, a capsule network-based approach for HAR via wearable sensors. SensCapsNet's architecture was created to handle spatial-temporal data through wearable sensors. The suggested network outperformed CNN and long short term memory (LSTM) techniques in experiments. The proposed CapsNet architecture's performance was evaluated by varying the dynamic routing among capsule layers. At the end, the outcomes of the suggested work has attained higher F1- score and improved accuracy values.

In 2020, Lv et al. [6] has introduced a unique hybrid deep learning network for HAR that similarly uses multimodal sensor data; nevertheless, the proposed approach was a ConvLSTM pipeline that fully utilizes the information retrieved throughout the temporal domain in each layer. To guarantee the maximal information flow across network levels, a dense connection module(DCM) was developed. The multilayer feature aggregation module(MFAM) output was fed into 2 LSTM layers of the temporal relationships. Lastly, the probability of each class was computed using a softmax function and a fully connected layer. The suggested model's efficacy was shown on 2 test datasets: UniMiB-SHAR and Opportunity. The findings demonstrate that the built network outperformed the most recent models.

In 2020, Ye et al. [7] have developed a novel probabilistic approach for HAR. In particular, these method has developed an ideal collection of latent patterns so that their temporal frameworks were important in detecting various human behaviour. Moreover, a new probabilistic First-Take-All (Pfta) method was suggested to create compact features, and the Hamming distance among compact features was used to efficiently measure the temporal structural similarity among various patterns. The suggested approach was further assessed in a public RGBD HAR dataset and it achieved competitive efficiency and accuracy.

In 2019, Singh et al. [8] have presented an approach for describing view-invariant human behavior. The suggested framework's components were three successive modules: (i) the identification and location of the background subtraction of human (ii) function extraction, and (iii) the end activity was linked by employing a collection of Hidden Markov Models (HMMs). In the suggested technique for activity representation, uniform rotation local binary patterns, a combination of optical flow-based motion feature, and contour-based distance signal feature was employed during the feature extraction process. According to the test analysis and findings of the selected datasets, the suggested framework was

resilient, adaptable, and efficient in terms of multiple perspectives activity recognition, size, and phase changes..

B. Review

Table 1 illustrates the review on HAR methods. Initially, the Kanade Lucas Tomasi (KLT) optical flow approach was determined in [1], that provides higher credibility degree, and better recognition performance; however, the major issue in the proposed model was the computing complexity. Moreover, the Machine Learning (ML) algorithm was deployed in [2] that provide higher accuracy, maximum precision, and less hamming Loss. Nevertheless, need to exploit different types of dependencies among labels and label correlations. DNN model were exploited in [3] that offers better accuracy rate and higher F1-value, but need to extend the proposed model to other mobile sensing tasks. Likewise, CNN model was exploited in [4], which offers maximum accuracy, better recall, and high precision. However, need to tackle the complex activities in which the human interact with objects or with one another. SensCapsNet model was exploited in [5] that provide improved accuracy, high precision, larger recall, and maximum F1-score; however, different dynamic routing algorithms were not investigated. In addition, MFAM and DCM method was introduced in [6], which offers better efficiency, high precision and larger recall. However, need to conduct experiments on additional datasets. pFTA algorithm was suggested in [7] that offers higher accuracy, less Computational Cost, and better efficiency. However, it does not exploit the temporal dynamics. Finally, the HMMs model was implemented in [8], which offers higher accuracy, less error, larger recall, maximum specificity, and high precision, but the predicted activity does not include all the information. These challenges were considered based on HAR models in the present work effectively.

TABLE I. REVIEW ON TRADITIONAL HAR APPROACH: FEATURES AND CHALLENGES

Author [citation]	**Adopted scheme**	**Features**	**Challenges**
Hairui et al. [1]	KLT optical flow approach	❖ Better credibility degree ❖ Higher recognition performance	❖ The major issue in the proposed model was the computing complexity.
Manan et al. [2]	ML algorithm	❖ Higher accuracy ❖ Maximum precision ❖ Less hamming Loss	❖ Need to exploit different types of dependencies among labels and label correlations.
Zhen et al. [3]	DNN model	❖ Better accuracy rate ❖ Higher F1-value	❖ Need to extend the proposed model to other mobile sensing tasks.

Hazar et al. [4]	CNN model	❖ Maximum accuracy ❖ Better recall ❖ High precision	❖ Need to tackle the complex activities in which the human interact with objects or with one another.
Pham et al. [5]	SensCapsNet model	❖ Improved accuracy ❖ High precision ❖ Larger recall ❖ Maximum F1-score	❖ Different dynamic routing algorithms were not investigated.
Lv et al. [6]	MFAM and DCM method	❖ Better efficiency ❖ High precision ❖ Larger recall	❖ Need to conduct experiments on additional datasets.
Ye et al. [7]	pFTA Algorithm	❖ Higher accuracy ❖ Less Computational Cost ❖ Better efficiency	❖ It does not exploit the temporal dynamics.
Singh et al. [8]	HMMs model	❖ Higher accuracy ❖ Less error ❖ Larger recall ❖ Maximum specificity ❖ High precision	❖ The predicted activity does not include all the information.

III. OVERVIEW OF THE ADOPTED HAR FRAMEWORK

This paper intends to introduce a new human activity recognition model and it involves three processes like

(1) Pre-processing
(2) Feature Extraction and
(3) Classification

- ✓ Initially pre-processing takes place, where the input data undergoes with process like background subtraction.
- ✓ The pre-processed data are then subjected to feature extraction process, in which an improved hierarchy of skeleton, weighted bag of Visual words, and Local Texton XOR patterns are extracted, and these are considered as features.
- ✓ Once the features are extracted, they are subjected to classification process in which the Optimized DBN is exploited.

- ✓ For more precise detection, the weight of DBN is optimally tuned by the proposed PRDO model that is the hybridized form of Poor and Rich Optimization (PRO) and deer hunting optimization (DHO) Algorithm.

The framework of the adopted HAR model is manifested in Fig.1.

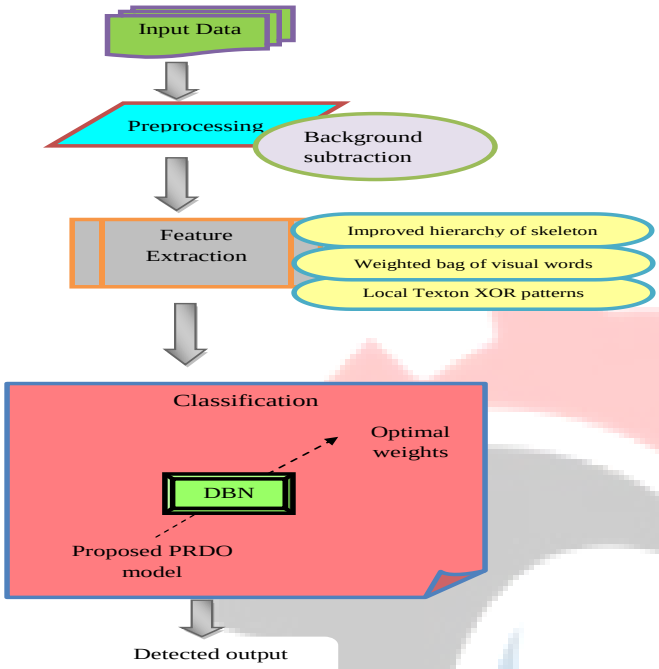

Fig. 1. Architecture of proposed HAR model

IV. PRE-PROCESSING AND FEATURE EXTRACTION FOR HAR

A. Preprocessing via Background Substraction

Background subtraction [39] is a method that involves creating a foreground mask to separate foreground items from the background. Moreover, the foreground mask is calculated through the background subtraction via subtracting the recent frame from a background model that includes the static component of the picture. There are two basic phases in background modelling:

- ✓ Background Initialization.
- ✓ Background Update.

The background's initial model is calculated in the 1st phase, and the changes in the scene is updated in the 2nd step. This method is used to detect dynamically moving objects from still images. The background removal approach is crucial for object tracking. The pre-processed frames are denoted as F^{pre}.

B. Feature extraction phase

Moreover, the preprocessed image F^{pre}` is subjected to extract the features that includes

- ❖ Weighted BovW

- Local Texton XOR patterns
- Improved hierarchy of skeleton

These features are determined as follows:

(i)Weighted BovW: The BovW is the concept which is gained in the textual information retrieval field. The BovW technique consists of two steps: “dictionary construction and a BovW formation histogram based on the dictionary”.

In the weighted BovW, the visual words are extracted from the given input foreground objects and the weights are assigned to each visual words according to this importance.

$$w_{u,v} = t_{u,v} * \log\left(\frac{M}{d_u + 1}\right) \quad (1)$$

In Eq. (1), $t_{u,v}$ indicates the number of occurrences of a word u in a image v, d_u denotes the number of images containing word u, and M refers to the documents or image count in the database. The extracted weighted Bovw based features is denoted as F^{BovW}.

(ii)Local Texton XOR patterns [30]: Moreover, the 7 dissimilar Texton shapes are used for the generation of texton image. Fig. 2 illustrates the texton shapes

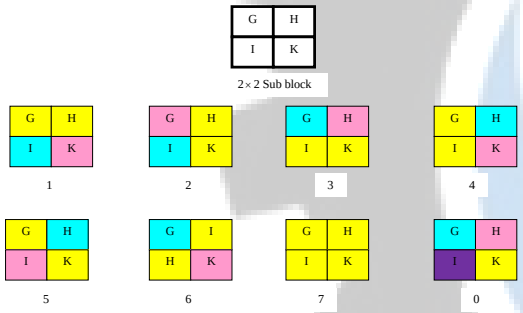

Fig. 2. Texton shapes

Here, the image is splitted into overlapping 2×2 subblocks known as J_1. The gray value positions are regarded as G, H, I, K for analysis. On the basis of texton shape, the subblocks are coded in Eq. (2).

$$Tx(Y,Z) = \begin{cases} 1,\ J_1(G) = J_1(H) \,\&\, J_1(I) \neq J_1(K) \\ 2,\ J_1(H) = J_1(K) \,\&\, J_1(G) \neq J_1(I) \\ 3,\ J_1(I) = J_1(K) \,\&\, J_1(G) \neq J_1(H) \\ 4,\ J_1(G) = J_1(I) \,\&\, J_1(H) \neq J_1(K) \\ 5,\ J_1(G) = J_1(K) \,\&\, J_1(H) \neq J_1(I) \\ 6, J_1(H) = J_1(I) \,\&\, J_1(G) \neq J_1(K) \\ 7, J_1(G) = J_1(H) \,\&\, J_1(I) = J_1(K) \\ 0, J_1(G) \neq J_1(H) \,\&\, J_1(I) \neq J_1(K) \end{cases} \quad (2)$$

For each pixel, the surrounding neighbors and its center is collected on the texton image. It achieved the XOR operation among the neighbor and center texton once after computing the texton image. Further, the local texton XOR patterns are determined in Eq. (3).

$$LTxXOR_{\tilde{P},\tilde{R}} = \sum_{i=1}^{\tilde{P}} 2^{(i-1)} \times f_3\left(Tx(h_i) \otimes Tx(h_c)\right) \quad (3)$$

Where, $f_3(y \otimes z) = \begin{cases} 1 & y \neq z \\ 0 & else \end{cases}$ (4)

In Eq. (3), $\otimes$ refers to the XOR operation among the variables, $Tx(h_c)$ indicates the texton shape for the center pixel h_c, and $Tx(h_i)$ denotes the texton shape for the neighbor pixel h_i.

In addition, the specified texton image is converted to LTxXORP maps within 0 to $2^p - 1$. Following the LTxXORP calculation, the total map is determined via constructing a histogram in Eq. (5).

$$His_{LTxXORP}(m) = \sum_{j=1}^{T_1}\sum_{k=1}^{T_2} f_2\left(LTxXORP(j,k), m\right);\ m \in \left[0, \left(2^p - 1\right)\right]$$

(5)

Fig. 3 represents the LTxXORP for an image. . The extracted LTxXORP features are denoted as $F^{LTxXORP}$.

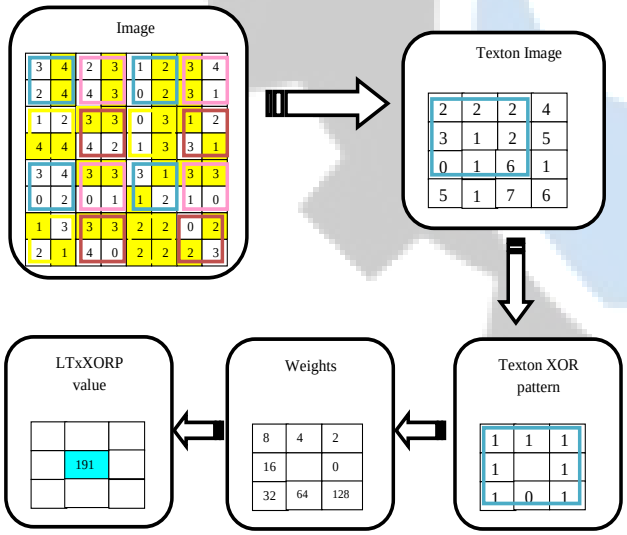

Fig. 3. Sample calculation of LTxXORP for an image

(iii)Improved hierarchy of skeleton: In conventional hierarchy of skeleton, a 3×3 subblocks of images is used. As per an improved hierarchy of skeleton, the 5×5 image sub blocks are used. Fig. 4 illustrates the Hierarchy of skeleton (a) Conventional (b) proposed subblocks of an image.

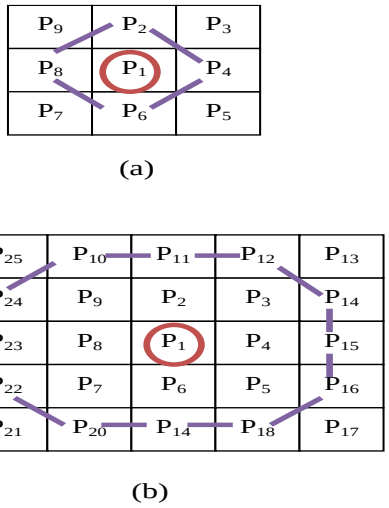

Fig. 4. Hierarchy of skeleton (a) Conventional (b) proposed subblocks of an image

Redundancy line removal: Moreover, the redundancy line is obtained through acute angle. It involves following steps as follows.

- Traverse each pixel of the image.
- If that point for target turn to (3) judge next point.
- Judge the count of target's 8-neighbour pixel only if it is 3 into (4), else review the next point.
- Individually compute the lines length as its 3 vertex was taken from (3).
- Set the maximum length value and proceeds only if the length is smaller than that value.

Moreover, the extracted improved hierarchy of skeleton features is denoted as F^{IHS}. Finally, the overall extracted features are $F = F^{BovW} + F^{LTxXORP} + F^{IHS}$.

V. CLASSIFICATION VIA OPTIMIZED DBN CLASSIFIER

The extracted features F are provided as the input for the classification phase via optimized DBN.

A. Optimizied DBN

DBN [38] with multiple layers consists of a visible and hidden neuron in each layer. The visible neurons are fully interconnected with the hidden neurons. In nature, the stochastic neuron's outcome is probabilistic in the Boltzmann networks. The DBN framework is an architectural model that includes hidden and visible neurons, as well as numerous layers that make up the output layer.

The output of neurons is probabilistic in the Boltzmann network. The output $\hat{o}$ is based on the probability function $Q(\psi)$ in Eq. (6). The probability function has used the sigmoid-shaped function.

$$\hat{o} = \begin{Bmatrix} 1 & with\ Q(\psi) \\ 0 & with\ 1-Q(\psi) \end{Bmatrix} \quad (6)$$

$$Q(\psi) = \frac{1}{1+e^{\frac{-\psi}{q}}} \quad (7)$$

The DBN approach is determined in Eq. (8), in which, q indicates the pseudo-temperature.

$$\lim_{q\to 0^+} Q(\psi) = \lim_{q\to 0^+} \frac{1}{1+e^{\frac{-\psi}{q}}} = \begin{cases} 0 & for \quad \psi < 0 \\ \frac{1}{2} & for \quad \psi = 0 \\ 1 & for \quad \psi > 0 \end{cases} \qquad (8)$$

The feature processing course is occured using a group of RBM layers in DBN structure and the classification occurs via MLP. The Boltzmann machine energy in the form of binary state s or neuron is determined in Eq. (9) and Eq. (10). Where, $W_{a,b}$ refers to the weights between the neurons that is optimally tuned via the new PRDO model and γ_a specifies the biases.

$$C(\hat{s}) = -\sum_{a<b} \hat{s}_a W_{a,b} - \sum_a \gamma_a \hat{s}_a \qquad (9)$$

$$\Delta C(\hat{s}_a) = \sum_b \hat{s}_a W_{a,b} + \gamma_a \qquad (10)$$

The development of energy based on joint composition in hidden and visible neurons $(\tilde{c}, \tilde{f})$is determined in Eq. (11), Eq. (12) and Eq. (13), where, $\tilde{f}_a$ and $\tilde{c}_a$ denotes the binary state of hidden unit b and a are the isible unit. $W_{a,b}$ specifies the weight and U_a and V_b refers to the biases.

$$C(\tilde{c}, \tilde{f}) = -\sum_{(a,b)} W_{a,b} \tilde{c}_a \tilde{f}_b - \sum_a U_a \tilde{c}_a - \sum_b V_b \tilde{f}_a \qquad (11)$$

$$\Delta C(\tilde{c}_a, \tilde{f}) = \sum_b W_{a,b} \tilde{f}_b + U_a \qquad (12)$$

$$\Delta C(\tilde{c}, \tilde{f}_b) = \sum_a W_{a,b} \tilde{c}_a + V_b \qquad (13)$$

The RBM training achieved the dispersed probabilities and the resultant weight allocations as given in Eq. (14). RBM method with probability distribution for the visible and hidden vectors pair $(\tilde{c}, \tilde{f})$ is specified in Eq. (15). Moreover, the partition function X is given in Eq. (16).

$$\hat{W}_{(a)} = \max_{\hat{W}} \prod_{\tilde{c}\in\hat{I}} D(\tilde{c}) \qquad (14)$$

$$D(\tilde{b}, \tilde{f}) = \frac{1}{X} e^{-C(\tilde{c}, \tilde{f})} \qquad (15)$$

$$X = \sum_{\tilde{c}, \tilde{f}} e^{-C(\tilde{c}, \tilde{f})} \qquad (16)$$

DBN scheme utilize the CD learning approach and the steps in CD method are given as follows.

- ✓ Pick the training samples $\tilde{f}$ and fix it to visible neurons.
- ✓ Compute the probability of hidden neurons $D_{\tilde{f}}$ via differentiating the product of visible vector s and $\hat{w}$ weight matrix as $D_{\tilde{f}} = \lambda(\tilde{c}.\hat{W})$, and it is given in Eq. (17), in which, λ denotes the activation function.

$$D\left(\tilde{f}_b \to 1 \mid \tilde{c}\right) = \lambda\left(V_b + \sum_a b_d W_{a,b}\right) \quad (17)$$

- ✓ The hidden states $\tilde{f}$ from $D_{\tilde{f}}$ probability are determined.
- ✓ Compute the exterior vectors product $\hat{s}$ and $D_{\tilde{f}}$ as positive gradient $\phi^+ = \tilde{c}.D_{\tilde{f}}^q$.
- ✓ The restoration of s' visible states from $\tilde{f}$ hidden states is defined in Eq. (18). Further more, it is essential to analyze hidden states f' from the c' restoration.

$$D\left(\tilde{c}_b \to 1 \mid \tilde{f}\right) = \lambda\left(U_a + \sum_a s_b W_{a,b}\right) \quad (18)$$

- ✓ Examine the exterior product c' and f', using its negative gradient $\phi^- = c'.f'^q$.
- ✓ The updated weight is defined in Eq. (19) in which, κ refers to the learning rate.

$$\Delta\hat{W} = \kappa\left(\phi^+ - \phi^-\right) \quad (19)$$

- ✓ The weight update is determined in Eq. (20) with new values.

$$W'_{a,b} = \Delta W_{a,b} + W_{a,b} \quad (20)$$

In the MLP model, assign $\left(B^P, A^P\right)$ training patterns. here, $1 \le P \le O$, P refers to the number of training patterns, A^P and B^P determines the predicted and actual output, correspondingly. Moreover, the error evaluation is given in Eq. (21). The output of DBN is denoted as CL_{DBN}.

$$e^P = B^P - A^P \quad (21)$$

VI. WEIGHT OPTIMIZATION VIA POOR AND RICH WITH DEER OPTIMIZATION ALGORITHM

A. Solution Encoding and Objective Function

As mentioned above, the weights of DBN are optimally tuned by the proposed PRDO method. Fig. 5 illustrates the input solution given to the proposed PRDO model. Here, the total number of weights in LSTM is indicated as N. The objective function of the implemented method is determined in Eq. (22), in which e^P is specified in Eq. (21).

$$Obj = \min\left(e^P\right) \quad (22)$$

Fig. 5. Solution Encoding

B. Proposed PRDO model

Even though, the existing DHO [32] provides better convergence behaviour and solved the entire test

problems, it is difficult to identify the local optimum points in the search spaces. In this work, DHO is combined with PRO [31] to propose the new model named as PRDO. Generally, the hybrid optimization schemes are supposed to be more suitable for particular search problems [33]. Although the primary goal of the suggested algorithm is to locate the best position for a person for hunting a deer, and required to observe the deer's behaviour. They possess particular features that enable attackers' complicated for hunting the deer. The visual power is 5 times higher than humans. The steps of the DHO are described as follows.

(i) Population initialization: The most important step of the DHO model is the hunters' population initialization, and it is given in Eq. (23).

$$S = \{S_1, S_2, ..., S_l\}; \quad 1 < g \le l \qquad (23)$$

In Eq. (23), l is the total count of hunters in the population S

(ii)Parametric initialization: The deer's position angle and the wind angle are initiated and these parameters are used for finding the best positions of the hunters. Moreover, the wind angle is calculated as the circle's circumference as the search space is measured as a circle. Moreover, the wind angle is given in Eq. (24).

$$\theta_n = 2\pi r \qquad (24)$$

Where, n refers to the current iteration and r denotes the random number within [0, 1]. Further, the deer's position angle is specified in Eq. (25). Where, θ is the wind angle.

$$\zeta_i = \theta + \pi \qquad (25)$$

(ii)Position propagation: As the location of the optimal space is undetermined at the beginning, this method considers the candidate solution that is nearest to the optimum, as defined by the fitness function, to be the best. Further, the two solutions are considered in this DHO model such as

- Leader position S^{lead} that is the hunter's 1st best position.
- Successor position S^{suc} that is the succeeding hunter's position.

(a) Propagation via a position of leader: Each individual in the population tries to obtain the best position once after defining the best positions, and begins the process of position updation. Here, the encircling behaviour is determined in Eq. (26).

$$S_{n+1} = S^{lead} - L.\hat{h}.\left|R \times S^{lead} - S_n\right| \quad (26)$$

where S_n is the position at the current iteration, S_{n+1} is the position at next iteration, L and R indicates the coefficient vectors and $\hat{h}$ is a random number in the wind speed from 0 to 2. However, as per the proposed PRDO method, coefficient vector L is determined as per Eq. (27). Further, the coefficient vector L is given in Eq. (28)

$$L = 2 \times rand * \frac{\hat{f}_{\hat{s}}}{\max \hat{f}_{\hat{s}}} \qquad (27)$$

$$R = 2.\tilde{u} \qquad (28)$$

In Eq. (28), $\tilde{u}$ is a random number among [0, 1].

(b) Propagation via position angle: The angle computation is necessary to calculate the hunter position in which the prey is ignorant to the attack and more effective in the hunting process. Further, the visualization angle of the prey or the deer is determined in Eq. (29).

$$\hat{a}_n = \frac{\pi}{8} \times r \qquad (29)$$

The parameter is computed on the basis of difference among the deer's visual angle and the wind angle, which helps to update the position angle.

$$\tilde{D}_n = \theta_n - \hat{a}_n \qquad (30)$$

For the next iteration, the position angle is given in Eq. (31).

$$\zeta_{n+1} = \zeta_n + \tilde{D}_n \qquad (31)$$

The position update by the position angle, and it is calculated in Eq. (32),

$$S_{n+1} = S^{lead} - \hat{h}.\left|\cos(\tilde{v}) \times S^{lead} - S_n\right| \qquad (32)$$

where $E = \zeta_{n+1}$, and S_n^* indicates the best position.

(iii) Propagation via the successor position: In the exploration phase, the encircling behavior is adopted via adjusting the vector R. Traditionally, the position is updated on the basis of successor position than the 1st best solution attained. However, as per the proposed logic, the updation can be done using PRO's updation function in Eq. (33),

$$S_{rich}^{new} = S_{rich,\hat{i}}^{old} + \tilde{r} * \left\lfloor S_{rich,best}^{old} - S_{poor,best}^{old} \right\rfloor + Levy(\beta) \qquad (33)$$

In Eq. (33), $S_{poor,best}^{old}$ refers to the position of the worst member in the rich population, $S_{rich,\hat{i}}^{old}$ indicates the current position of $\hat{i}^{th}$ member of the rich population, and $\tilde{r}$ specifies the pattern improvement parameter between 0 and 1. The pseudocode of the adopted PRDO scheme is given in Algorithm 1.

ALGORITHM 1: Adopted PRDO method	
Population initialization S	
1st best solution S^{lead} and 2nd best solution S^{suc}	
Begin	
while $(n < n\max)$	
	for each solution in the population
	Compute the fitness of each solution
	Update $\hat{a}$, $\tilde{D}$, E, $\hat{h}$, L, R and $\tilde{k}$
	if $(\hat{h} < 1)$
	if $(\lvert R \rvert \geq 1)$

		Update the position of the individual in Eq. (26)
	Else	
		Update the proposed position in Eq. (33)
	end if	
	Else	
		The position is updated in Eq. (32)
	end if	
	end for	
	Compute the fitness of each solution	
	Update S^{lead} and S^{suc}	
	$n = n + 1$	
	end while	
	Return S^{lead}	
Terminate		

VII. RESULTS AND DISCUSSION

A. Simulation procedure

The proposed HAR with DBN+PRDO model was implemented in PYTHON and their outcomes was verified. Moreover, the dataset has been collected from [29]. Dataset Description: “UCF-ARG (University of Central Florida-Aerial camera, Rooftop camera and Ground camera) Data set is a Multiview Human Action dataset. UCF-ARG includes 10 actions performed through 12 actors recorded from a ground camera, a rooftop camera at a height of 100 feet, and an aerial camera mounted onto the payload platform of a 13' Kingfisher Aerostat helium balloon. Except for Open-Close Trunk, all the other actions are performed 4 times by each actor in different directions. Open-Close Trunk is performed only 3 times, i.e. on 3 cars parked in different directions. The actions are captured using a high-definition camcorder (Sanyo Xacti FH1A camera) 1920 X 1080 at 60fps (frames per second)”. The sample images are illustrated in Fig. 6. Further, the proposed DBN+PRDO model over the existing models like Linear SVM [26], SVM [27], SOEHM+ hybrid classifier [28], RNN [34], LSTM [35], DBN [38], DBN + MFO [37], DBN + GOA [36], DBN + DHO [32], and DBN+ PRO [31], respectively with respect to certain measures

like NPV, accuracy, FNR, sensitivity, F-measure, FPR, specificity, MCC, and precision for different learning percentages like 60, 70, 80, and 90.

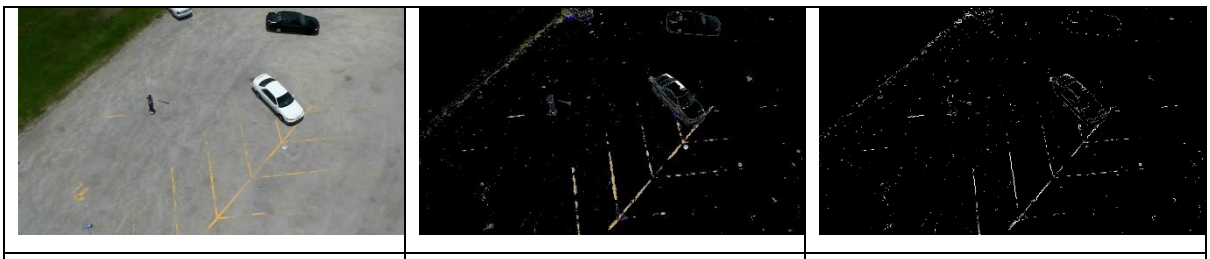

(i) (ii) (iii)

Fig. 6. Sample images (i) Original image, (ii) Back ground substracted image, and (iii) image

B. **Performance Analysis**

The performance analysis of the presented DBN+PRDO scheme is computed to the existing schemes like Linear SVM, SVM, SOEHM+ hybrid classifier, RNN, LSTM, DBN, DBN + MFO, DBN + GOA, DBN + DHO, and DBN+ PRO, respectively in terms of certain metrics, and it is illustrated in Fig. 7, 8, and 9. Moreover, the accuracy of the adopted DBN+PRDO scheme for learning percentage 70 is 35.36%, 23.1%, 2.08%, 33.73%, 42.75%, 48.71%, 9.22%, 10.11%, 10.34%, and 9.65% superior than the existing schemes like Linear SVM, SVM, SOEHM+ hybrid classifier, RNN, LSTM, DBN, DBN + MFO, DBN + GOA, DBN + DHO, and DBN+ PRO, correspondingly as shown in Fig. 7(b). This proves that the accuracy of adopted work is larger than the traditional models. Likewise, the adopted DBN+PRDO scheme attains higher sensitivity (~0.94) for learning percentage 60 in human activity detection than other existing schemes in Fig. 7(a). In addition, the precision as well as specificity of the presented DBN+PRDO scheme is also found to be higher for every variation in learning percentages than existing models like Linear SVM, SVM, SOEHM+ hybrid classifier, RNN, LSTM, DBN, DBN + MFO, DBN + GOA, DBN + DHO, and DBN+ PRO, respectively. This analysis results have shown the impact of proposed concept, which gets trained with the appropriate features. Moreover, as the DBN weights are tuned optimally, it paves the way for better recognition results with minimization of errors.

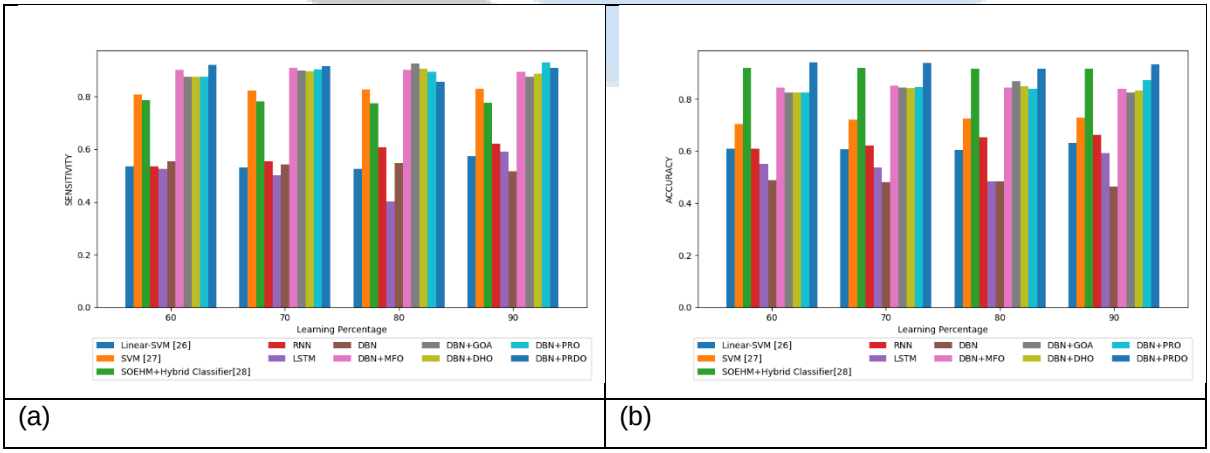

(a) (b)

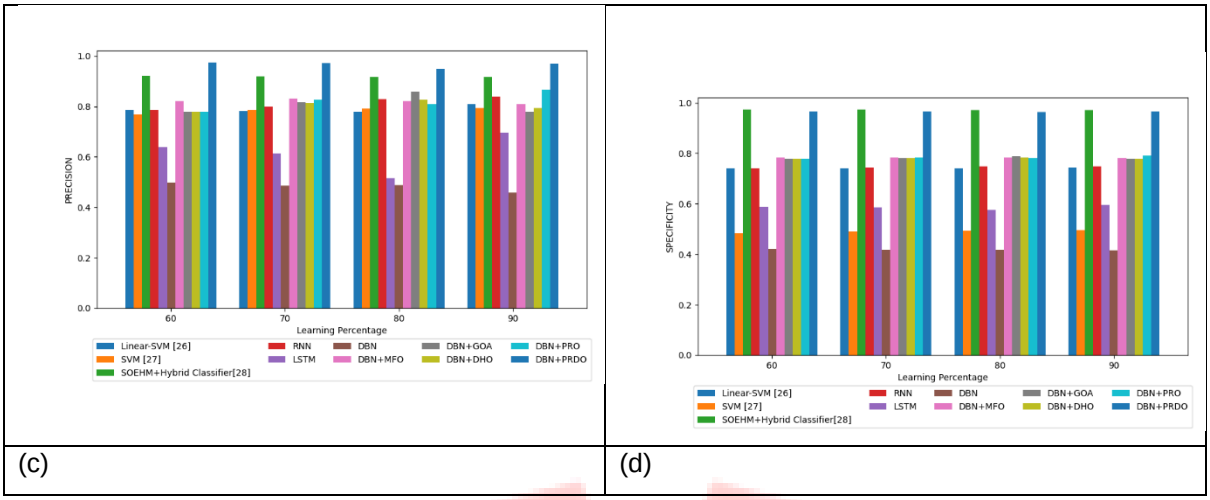

(c) (d)

Fig. 7. Performance analysis of the proposed scheme over the traditioanl models for (a) sensitivity (b) accuracy (c) precision (d) specificity

Fig. 8 represents the negative metrics like FPR, and FNR of the presented DBN+PRDO model over other conventional schemes like Linear SVM, SVM, SOEHM+ hybrid classifier, RNN, LSTM, DBN, DBN + MFO, DBN + GOA, DBN + DHO, and DBN+ PRO, respectively. Minimum FNR (~0.083) value of proposed work proves that the model is less prone to error, which leads to precise prediction results for learning percentage 70 (Fig. 8(a)). The FPR of the presented DBN+PRDO model is 0.03439 at 90th learning percentage, which is the least value when comported over other conventional schemes like Linear SVM, SVM, SOEHM+ hybrid classifier, RNN, LSTM, DBN, DBN + MFO, DBN + GOA, DBN + DHO, and DBN+ PRO, respectively. Deviation in learning percentage shows the difference in the performance. This has proved that the model with optimal weights ensures minimized error by the adopted optimization model.

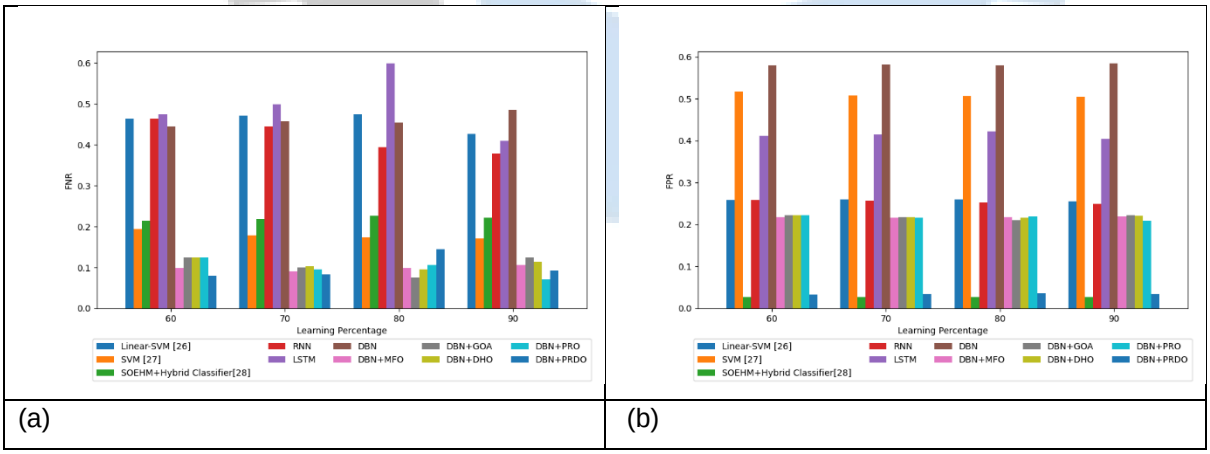

(a) (b)

Fig. 8. Performance analysis of the proposed scheme over the traditioanl models for (a) FNR (b) FPR

Fig. 9 illustrates the other measures analysis such as NPV, MCC, and F-measure of the adopted DBN+PRDO model than other existing models. Likewise, the F-measure of adopted DBN+PRDO model for learning percentage 60 in Fig. 9(b) is superior to other traditional scheme like Linear SVM, SVM, SOEHM+ hybrid classifier, RNN, LSTM, DBN, DBN + MFO, DBN + GOA, DBN + DHO, and DBN+ PRO, correspondingly. From the graph, it is shown clearly that the NPV of the adopted DBN+PRDO model

holds a higher value (~0.898) for learning percentage 90; whereas, the compared existing models like Linear SVM, SVM, SOEHM+ hybrid classifier, RNN, LSTM, DBN, DBN + MFO, DBN + GOA, DBN + DHO, and DBN+ PRO, respectively attains lower values as per Fig. 9(a). Similarly, the adopted DBN+PRDO model attains highest MCC (~0.877) for learning percentage 70 when compared to the training percentage 90 in Fig. 9(c). Thus, the performance of presented DBN+PRDO model has shown its enhancement over other existing schemes.

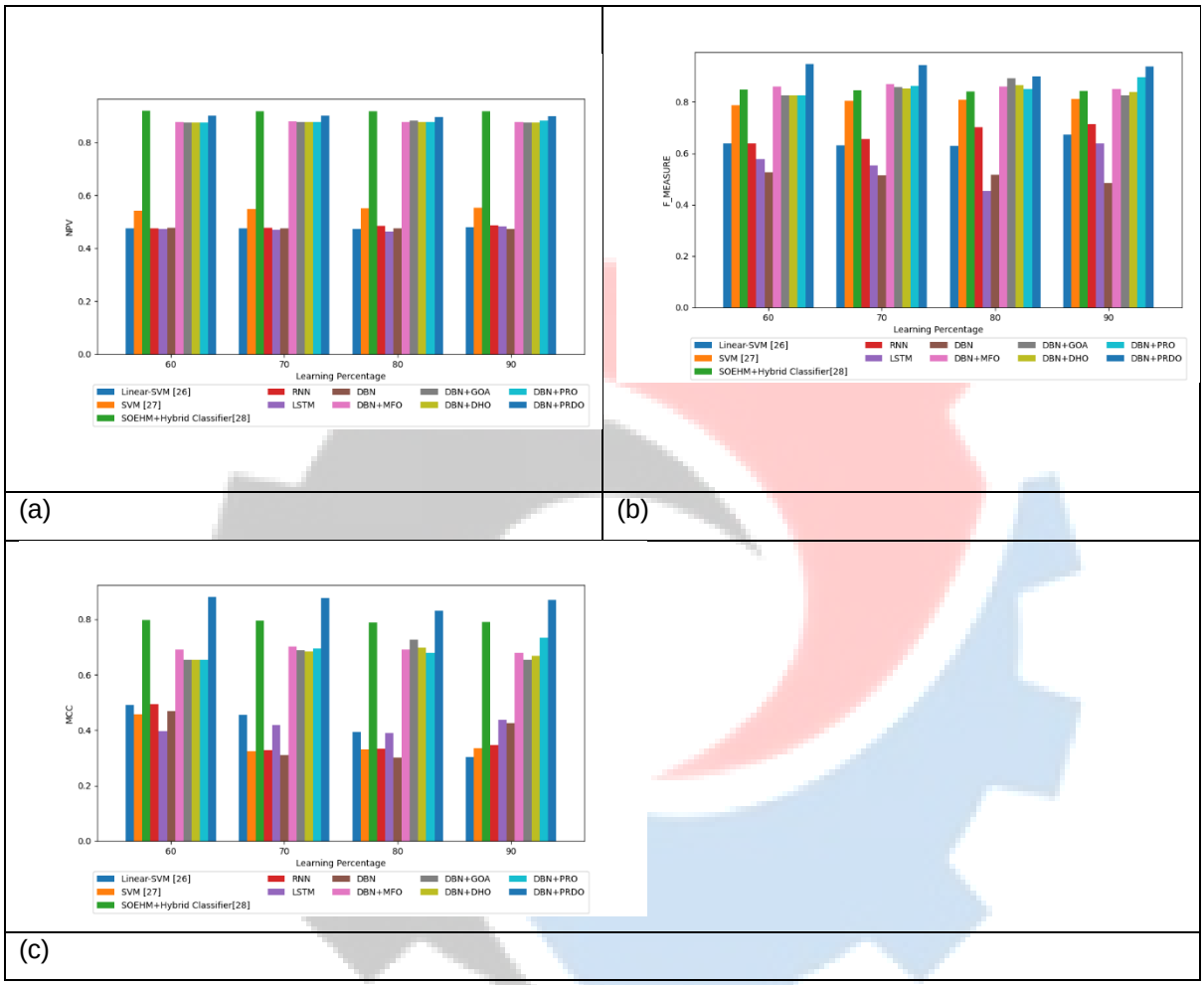

Fig. 9. Performance analysis of the proposed scheme over the traditioanl models for (a) NPV (b) F-measure (c) MCC

C. **Overall Performance Evaluation**

The overall performance of the adopted DBN+PRDO model with respect to various metrics in manifested in Table II. On observing the table, the adopted DBN+PRDO model have proven its recognition ability than other conventional models such as Linear SVM, SVM, SOEHM+ hybrid classifier, RNN, LSTM, DBN, DBN + MFO, DBN + GOA, DBN + DHO, and DBN+ PRO, respectively. Furthermore, the proposed DBN+PRDO model attains maximum accuracy values (~0.938093) when compared to the existing models. Likewise, the proposed DBN+PRDO model attains better MCC than other traditional models like Linear SVM, SVM, SOEHM+ hybrid classifier, RNN, LSTM, DBN, DBN + MFO, DBN + GOA, DBN + DHO, and DBN+ PRO, correspondingly. The adopted DBN+PRDO model

holds lower FPR value with better performance than other traditional models like Linear SVM, SVM, SOEHM+ hybrid classifier, RNN, LSTM, DBN, DBN + MFO, DBN + GOA, DBN + DHO, and DBN+ PRO, respectively in Table II. The outcomes have summarized that the adopted DBN+PRDO model performance is improved over the conventional models.

TABLE II. OVERALL PERFORMANCE ANALYSIS OF THE ADOPTED AND EXISTING WORKS

Measures	Linear-SVM [26]	SVM [27]	RNN [34]	LSTM [35]	DBN [38]	DBN+ MFO [37]	DBN+ GOA [36]	DBN+ DHO [32]	DBN+ PRO [31]	Proposed DBN+PRDO model
Sensitivity	0.529716	0.822094	0.555556	0.501355	0.542929	0.908501	0.899468	0.89696	0.904172	0.91638
Specificity	0.740286	0.491304	0.742638	0.585291	0.418733	0.784144	0.782061	0.781541	0.783102	0.966006
Accuracy	0.606388	0.720974	0.621635	0.537564	0.481145	0.851518	0.843198	0.841001	0.847449	0.938093
Precision	0.780793	0.785892	0.798096	0.614422	0.485475	0.832673	0.817657	0.813531	0.825446	0.971954
F-measure	0.631203	0.803585	0.655097	0.55216	0.512597	0.868936	0.856614	0.853211	0.863018	0.943349
MCC	0.454729	0.323828	0.329254	0.420109	0.309654	0.701978	0.688284	0.684549	0.695365	0.877086
NPV	0.474064	0.548713	0.477124	0.471036	0.47559	0.878762	0.877449	0.877121	0.878105	0.899863
FPR	0.259714	0.508696	0.257362	0.414709	0.581267	0.215856	0.217939	0.218459	0.216898	0.033994
FNR	0.470284	0.177906	0.444444	0.498645	0.457071	0.091499	0.100532	0.10304	0.095828	0.08362

D. **Statistical Analysis**

The statistical analysis of the presented DBN+PRDO model is computed to the existing scheme in terms of accuracy measure is represented in Table III. Naturally, the meta-heuristic algorithms are stochastic; thus, the algorithms are executed for several times for determining the achievement of the defined objective. The mean performance of the adopted DBN+PRDO approach holds better outcomes (~0.932101) than other traditional models like Linear SVM, SVM, SOEHM+ hybrid classifier, RNN, LSTM, DBN, DBN + MFO, DBN + GOA, DBN + DHO, and DBN+ PRO, correspondingly. The best case scenario proves the betterment of proposed work with accurate results than the other existing models. Thus, the proposed work has proved its betterment by recognizing the human activity. Therefore, the improvement of the adopted DBN+PRDO scheme has been effectively validated.

TABLE III. STATISTICAL ANALYSIS WITH RESPECT TO ACCURACY: PROPOSED VS. CONVENTIONAL MODELS

Metrics	Linear-SVM [26]	SVM [27]	RNN [34]	LSTM [35]	DBN [38]	DBN+ MFO [37]	DBN+ GOA [36]	DBN+ DHO [32]	DBN+ PRO [31]	Proposed DBN+PRDO model
Mean	0.613403	0.719683	0.636889	0.541642	0.479537	0.845242	0.839831	0.836326	0.84576	0.932101
Median	0.608335	0.723431	0.637317	0.544877	0.482147	0.845347	0.833661	0.836349	0.843102	0.936059

Standard deviation	0.011237	0.009988	0.021583	0.038657	0.009019	0.004514	0.017967	0.009219	0.017653	0.009366
Worst	0.60442	0.703076	0.610282	0.484424	0.46476	0.838755	0.824124	0.824124	0.824124	0.916313
Best	0.632521	0.728796	0.662642	0.592393	0.489096	0.851518	0.867876	0.848483	0.872712	0.939974

E. **Analysis based on features**

The analysis of proposed work based on features is illustrated in Table IV. In addition, the proposed features (improved hierarchy of skeleton, weighted Bovw, and Local Texton XOR patterns) + DBN + Proposed PRDO model hold better MCC than the conventional features (hierarchy of skeleton, weighted Bovw, and Local Texton XOR patterns) without optimization and with optimization. Further, the accuracy of proposed features + DBN + Proposed PRDO model has shown (~0.939974) than other conventional features without optimization and with optimization. Similar performance is observed with respect to all other measures. This analysis results have shown the impact of proposed features + DBN + Proposed PRDO model aids well to recognize the human activity more accurately, whereas the conventional features without optimization and with optimization shows its poor performance with the proposed concept. This absolutely shown that the proposed combination is fit for the HAR model.

TABLE IV. ANALYSIS OF PROPOSED WORK WITH DIFFERENT FEATURE COMBINATIONS

Metrics	**Conventional features + without Optimization**	**Conventional features + with optimization**	**Proposed features+ DBN +Proposed PRDO model**
Sensitivity	0.486111	0.914384	0.920447
Specificity	0.412831	0.785711	0.966206
Accuracy	0.447696	0.857308	0.939974
Precision	0.429025	0.842587	0.973396
F-measure	0.455788	0.877018	0.946181
MCC	0.409535	0.711128	0.880207
NPV	0.469534	0.879747	0.900412
FPR	0.587169	0.214289	0.033794
FNR	0.513889	0.085616	0.079553

F. **Convergence Analysis**

The convergence of the presented PRDO model and the traditional schemes is assessed by altering the iteration count from 0, 5, 10, 15, 20, and 25, correspondingly. Fig. 10 represents the convergence analysis of presented approach over the traditional approaches. The proposed PRDO approach attains

the minimum cost function as per the defined objectives in Eq. (22). As the count of iteration rises, the cost function of PRDO algorithm gets minimized. Particularly, the cost function of proposed PRDO model had a fall in between the range 10th to 13th iterations and then it remains constant up to 25th iteration. The cost function of the adopted PRDO scheme provides lower value (2.291) at the 20th iteration than other existing models like MFO, GOA, DHO, and PRO, correspondingly. Further, the cost function of the adopted PRDO scheme attains reduced cost values with better performance at the 15th iteration when compared to the other techniques. Thus, it is shown clearly that the adopted PRDO approach had attained the least cost function with superior outcomes.

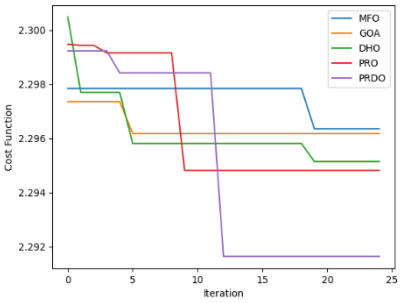

Fig. 10. Convergence analysis of proposed approach and existing approaches

VIII. CONCLUSION

This paper has introduced a new HAR model and it involves three process like “(1) Pre-processing, (2) Feature Extraction and (3) Classification”. The pre-processing of input data was done via background subtraction. The pre-processed data were subjected to extract the features, in which an improved hierarchy of skeleton, weighted bag of Visual words, and Local Texton XOR patterns were extracted. Based on the extracted features, the classification process takes place, in which the Optimized DBN was exploited. For more precise detection, the weight of DBN was optimally tuned via proposed PRDO model. Finally, performance of the presented model was computed over the conventional techniques with respect to various performance metrics. From the graph, the accuracy of the adopted DBN+PRDO scheme for learning percentage 70 was 35.36%, 23.1%, 2.08%, 33.73%, 42.75%, 48.71%, 9.22%, 10.11%, 10.34%, and 9.65% superior than the existing schemes like Linear SVM, SVM, SOEHM+ hybrid classifier, RNN, LSTM, DBN, DBN + MFO, DBN + GOA, DBN + DHO, and DBN+ PRO, correspondingly. Minimum FNR (~0.083) value of proposed work proves that the model was less prone to error, which leads to precise prediction results for learning percentage 70. Likewise, the proposed DBN+PRDO model attains better MCC than other traditional models like Linear SVM, SVM, SOEHM+ hybrid classifier, RNN, LSTM, DBN, DBN + MFO, DBN + GOA, DBN + DHO, and DBN+ PRO, correspondingly. The mean performance of the adopted DBN+PRDO approach holds better outcomes (~0.932101) than other traditional models like Linear SVM, SVM, SOEHM+ hybrid classifier, RNN, LSTM, DBN, DBN + MFO, DBN + GOA, DBN + DHO, and DBN+ PRO, correspondingly.

REFERENCES

[1] H. Jia, S. Chen, ”Integrated data and knowledge driven methodology for hu man activity recognition”, Information Sciences, Volume 536, 2020, pp. 409- 430.

[2] M. Jethanandani, A. Sharma, T. Perumal, J. Chang, ”Multi-label classi fication based ensemble learning for human activity recognition in smart home”, Internet of Things, Volume 12, 2020, pp. 100324.

[3] Z. Qin, Y. Zhang, S. Meng, Z. Qin, K. Choo, ”Imaging and fusing time series for wearable sensor-based human activity recognition”, Information Fusion, Volume 53, 2020, pp. 80-87.

[4] H. Mliki, F. Bouhlel, M. Hammami, ”Human activity recognition from UAV-captured video sequences”, Pattern Recognition, Volume 100, 2020, pp. 107140.

[5] C. Pham, S. Nguyen-Thai, H. Tran-Quang, S. Tran, H. Vu, T. Tran,T. Le, ”SensCapsNet: Deep Neural Network for Non-Obtrusive Sensing Based Hu man Activity Recognition”, : IEEE Access, Volume 8, 2020, pp. 86934– 86946.

[6] T. Lv, X. Wang, Y. Xiao, M. Song, ”A Hybrid Network Based on Dense Connection and Weighted Feature Aggregation for Human Activity Recog nition”, IEEE Access, Volume 8, 2020, pp. 68320-68332.

[7] J. Ye, G. -J. Qi, N. Zhuang, H. Hu, K. A. Hua, ”Learning Compact Features for Human Activity Recognition Via Probabilistic First-Take-All”, IEEE Transactions on Pattern Analysis and Machine Intelligence, Volume 42, 2020, pp. 126-139.

[8] R. Sing, A. K. S. Kushwaha, R. Srivastava , ”Multi-view recognition system for human activity based on multiple features for video surveillance system”, Multimedia Tools and Applications, Volume 78, 2019, pp. 17165–17196.

[9] R. Li, H. Li, W. Shi, ”Human activity recognition based on LPA”, Multi media Tools and Applications, Volume 79, 2020, pp. 31069–31086.

[10] A. Khelalef F. Ababsa, N. Benoudjit, ”An Efficient Human Activity Recog nition Technique Based on Deep Learning”, Pattern Recognition and Image Analysis, Volume 29, 2019, pp. 702–715.

[11] A. Lentzas D. Vrakas, ”Non-intrusive human activity recognition and ab normal behavior detection on elderly people: a review”, Artificial Intelli gence Review, Volume 53, 2020, pp. 1975–2021.

[12] S. A. Khowaja B. N. Yahya, S. Lee, ”CAPHAR: context-aware personal ized human activity recognition using associative learning in smart environ ments”, Human-centric Computing and Information Sciences, Volume 10, 2020, pp. 35.

[13] D. G. Shreyas, S. Raksha, B. G. Prasad, ”Implementation of an Anomalous Human Activity Recognition System”, SN Computer Science, Volume 1, 2020, pp. 1-10.

[14] A. Ladjailia, I. Bouchrika, H. F. Merouani, N. Harrati, Z. Mahfouf, ”Hu man activity recognition via optical flow: decomposing activities into basic actions”, Neural Computing and Applications, Volume 32, 2020, pp. 16387– 16400.

[15] M. Inoue, S. Inoue, T. Nishida, ”Deep recurrent neural network for mo bile human activity recognition with high throughput”, Artificial Life and Robotics, Volume 23, 2018, pp. 173–185.

[16] P. Asghari, E. Soleimani, E. Nazerfard, ”Online human activity recognition employing hierarchical hidden Markov models”, Journal of Ambient Intelligence and Humanized Computing, Volume 11, 2020, pp. 1141–1152.

[17] D. Thakur, S. Biswas, ”Smartphone based human activity monitoring and recognition using ML and DL: a comprehensive survey”, Journal of Ambient Intelligence and Humanized Computing, Volume 11, 2020, pp. 5433–5444.

[18] D. Hooda, R. Rani, ”Ontology driven human activity recognition in hetero geneous sensor measurements”, Journal of Ambient Intelligence and Humanized Computing, Volume 11, 2020, pp. 5947–5960.

[19] S. V. Shojaedini, M. J. Beirami, ”Mobile sensor based human activity recog nition: distinguishing of challenging activities by applying long short-term memory deep learning modified by residual network concept”, Biomedical Engineering Letters, Volume 10, 2020, pp. 419–430.

[20] H. Naveed, G. Khan, A. U. Khan, A. Siddiqi, M. U. G. Khan, ”Human activity recognition using mixture of heterogeneous features and sequential minimal optimization”, International Journal of Machine Learning and Cybernetics, Volume 10, 2019, pp. 2329–2340.

[21] M. M. Hassan, S. Huda, M. Z. Uddin, A. Almogren, M. Alrubaian, ”Human Activity Recognition from Body Sensor Data using Deep Learning”, Journal of Medical Systems, Volume 42, 2018, pp. 99. [22] E. Casella, M. Ortolani, S. Silvestri, S. K. Das, ”Hierarchical syntactic models for human activity recognition through mobility traces”, Personal and Ubiquitous Computing, Volume 24, 2020, pp. 451–464.

[23] G. Mohmed, A. Lotfi, A. Pourabdollah, ”Enhanced fuzzy finite state ma chine for human activity modelling and recognition”, Journal of Ambient Intelligence and Humanized Computing, Volume 11, 2020, pp. 6077–6091.

[24] H. Yan, Y. Zhang, Y. Wang, K. Xu, ”WiAct: A Passive WiFi-Based Hu man Activity Recognition System”, IEEE Sensors Journal, Volume 20, 2020, pp. 296-305.

[25] I. A. Lawal, S. Bano, ”Deep Human Activity Recognition With Localisation of Wearable Sensors”, IEEE Access, Volume 8, 2020, pp. 155060–155070.

[26] M. V. Silva, A. N. Marana, ”Human action recognition in videos based on spatiotemporal features and bag-of-poses”, Applied Soft Computing, Volume 95, 2020, pp. 106513.

[27] I. P. Febin, K. Jayasree, P. T. Joy, ”Violence detection in videos for an intelligent surveillance system using MoBSIFT and movement filtering algorithm”, Pattern Analysis and Applications, Volume 23, 2020, pp. 611–623.

[28] B. Mahasseni, S. Todorovic, ”Regularizing Long Short Term Memory with 3D Human-Skeleton Sequences for Action Recognition”,IEEE Conference on Computer Vision and Pattern Recognition (CVPR), 2016, pp. 3054- 3062.

[29] A. Nagendran, D. Harper, M. Shah, University of Central Florida, 2010, http://Crcv.Ucf.Edu/Data/UCF-ARG.Php.

[30] A. Bala, T. Kaur, ”Local texton XOR patterns: A new feature descriptor for content-based image retrieval”, Engineering Science and Technology, an International Journal, Volume 19, 2016, pp. 101-112.

[31] S. H. S. Moosavi, V. K. Bardsiri, ”Poor and rich optimization algorithm: A new human-based and multi populations algorithm”, Engineering Appli cations of Artificial Intelligence, Volume 86, 2019, pp. 165-181.

[32] G. Brammya, S. Praveena, N. S. Preetha, R. Ramya, B. R. Rajakumar, D. Binu, ”Deer Hunting Optimization Algorithm: A New Nature-Inspired Meta-heuristic Paradigm”, The Computer Journal, Volume 86, 2019, pp. 1- 20.

[33] M. M. Beno, I. R. Valarmathi, S. Swamy, B. R. Rajakumar, ”Threshold prediction for segmenting tumour from brain MRI scans”, International Journal of Imaging Systems and Technology, Volume 24, 2014, pp. 129- 137.

[34] L. Kao, C. C. Chiu, ”Application of integrated recurrent neural network with multivariate adaptive regression splines on SPC-EPC process”, Journal of Manufacturing Systems, Volume 57, 2020, pp. 109-118.

[35] X. Zhou, J. Lin, Z. Zhang, Z. Shao, S. Chen, H. Liu, ”Improved itracker combined with bidirectional long short-term memory for 3D gaze estimation using appearance cues”, Neurocomputing, Volume 390, 2020, pp. 217-225. 57, 2020, pp. 109-118.

[36] S. Saremi, S. Mirjalili, A. Lewis, ”Grasshopper Optimisation Algorithm: Theory and application”,Advances in Engineering Software, Volume 105, 2017, pp. 30-47.

[37] S. Mirjalili, ”Moth-flame optimization algorithm: A novel nature-inspired heuristic paradigm”,Knowledge-Based Systems, Volume 89, 2015, pp. 228- 249.

[38] H. Z. Wang, G. B. Wang, G. Q. Li, J. C. Peng, Y. T. Liu, ”Deep be lief network based deterministic and probabilistic wind speed forecasting ap proach”,Applied Energy, Volume 182, 2016, pp. 80-93. [39] Background, Subatrction from, ”https://docs.opencv.org/3.4/d1/dc5/tutorial background subtraction.htm”, Access Date: 23-06-2021.

[40] P. M R, ”Improved Deer Hunting Optimization Algorithm for video based salient object detection”,Multimedia Research, Volume 3, 2020, pp. 1-11.

[41] M A. kumar, ”Texton Features and Deep Belief Network for Leaf Disease Classification”,Multimedia Research, Volume 3, 2020, pp. 1-8.

[42] R A. Nikam, ”A Novel Hybrid Approch for Optimal Reactive Power Dis patch under Unbalanced Conditions”,Journal of Computational Mechanics, Power System and Control, Volume 3, 2020, pp. 1-10.

[43] Y. Xu, ”Hybrid Grey Wolf Optimization and Cuckoo Search algorithm for UPQC positioning in power distribution network”,Journal of Computa tional Mechanics, Power System and Control, Volume 3, 2020, pp. 1-9.

[44] J. Wang, ”Hybrid Optimization Algorithm for multihop routing protocol in WSN”,Journal of Networking and Communication Systems, Volume 3, 2020, pp. 1-8.

[45] S. Rathod, ”Hybrid Metaheuristic Algorithm for Cluster Head Selection in WSN”,Journal of Networking and Communication Systems, Volume 3, 2020, pp. 1-9.